Molecular aggregations in water–2-butoxyethanol mixtures by ultrasonic and Brillouin light-scattering measurements

G. D'Arrigo
Dipartimento di Fisica, Università di Roma "La Sapienza," Piazzale Aldo Moro 2, I-00185 Roma, Italy

F. Mallamace
Dipartimento di Física, Università di Messina, I-98166 Villaggio Santa Agata, Casella Postale 55 (Messina), Italy

N. Micali
Istituto di Tecniche Spettroscopiche, I-98166 Villaggio Santa Agata, Casella Postale 55 (Messina), Italy

A. Paparelli
Dipartimento di Física, Università di Roma "La Sapienza," Piazzale Aldo Moro 2, I-00185 Roma, Italy

C. Vasi
Istituto di Tecniche Spettroscopiche, I-98166 Villaggio Santa Agata, Casella Postale 55 (Messina), Italy
(Received 11 March 1991)

By means of ultrasonic and Brillouin light-scattering techniques, we have performed extensive measurements of the attenuation coefficient and sound velocity in 2-butoxyethanol aqueous solutions over a large temperature range. In the more concentrated solutions, the frequency dependence of these properties is well accounted for by a double relaxation time equation thus excluding contributions from concentration fluctuations. This finding, as well as the overall behavior as a function of concentration and temperature, suggests the presence of alcohol aggregates beyond a characteristic concentration-temperature line resembling a critical micelle concentration curve in micellar systems. The similarity between the ultrasonic behavior and the type observed in nonionic surfactant aqueous solutions, as well as indications from other experimental sources, strongly supports the possibility that butoxyethanol aggregates are micellelike structures.

I. INTRODUCTION

The structural and dynamical properties of aqueous solutions of 2-butoxyethanol (BE) have been studied recently by various physicochemical techniques such as calorimetry [1,2], densimetry [2,3], ultrasonic spectroscopy [4-9], elastic, and quasielastic light scattering [8,10–12], and small-angle neutron scattering (SANS) [13]. These experiments support the presence of alcohol aggregates similar to micelles. The ability of BE amphiphilic molecules ($C_4H_9OC_2H_4OH$) to form topologically ordered surfactantlike aggregates is also suggested by their chemical structure and phase diagram [12], which are similar to those of long-chain nonionic surfactants $C_nH_{2n+1}(OCH_2CH_2)_mOH$ (polyoxyethylene monoalkyl ethers, usually denoted as C_nE_m). BE can be considered as a short (C_4E_1) homologous member of the C_nE_m series, so that one expects that static and dynamic properties of its aqueous solutions exhibit behaviors similar to those in the corresponding C_nE_m solutions.

The interest for BE solutions is manifold. It concerns the requirements for an amphiphilic molecule to be a surfactant. By increasing the hydrophobic alkyl chain length of simple alcohols (C_nE_0) and alkoxyethanols (C_nE_1) in solutions with water it seems that there are molecular aggregations changing from short-living fluctuating associations to microstructures having a well-defined surface of demarcation. Apart from some balance of hydrophilic and hydrophobic moities, there is evidence for the requirement of some minimal length of the alkyl chain to form ordered aggregations. In the sequence of C_nE_1 ethoxylated alcohols, BE molecules seem to have this minimal length.

A related interest to BE aqueous solutions comes from the oil recovery processes. In fact, the formation and stability of microemulsions can be enhanced by the presence of cosurfactants (long-chained alcohols).

In a previous paper [9] we presented ultrasonic absorption coefficient and velocity measurements in two concentrations of BE aqueous solutions. In light of recent structural and dynamical indications from SANS [13] and light scattering [12] experiments, this paper extends our ultrasonic investigations to a wider composition range and, in addition, we have performed Brillouin light-scattering (BLS) measurements. From these experiments we hope to gain a better understanding of the ultrasonic dynamics and the related aggregation processes over large temperature and concentration ranges.

II. EXPERIMENT

The samples preparation and the ultrasonic techniques used for absorption coefficient (α) and sound velocity (c)

measurements are described elsewhere [9,14]. The concentrations investigated in these experiments were $X_3=0.015$ and $X_4=0.050$ (where X is the molar fraction of BE) and they add to the previously studied $X_1=0.030$ and $X_2=0.090$. The α and c measurements have been performed in the frequency (f) ranges 5–250 and 5–95 MHz, respectively, and for temperatures extending from about 45 °C down to the solidification temperatures. The accuracy of the ultrasonic velocity is estimated to be ~0.1% at the lowest frequencies and ~0.2% at the highest. Depending on the frequency range, the accuracy of the ultrasonic attenuation, as expressed by α/f^2, is around 5–10 %.

The BLS experiments were made in five samples of composition $X=0.015$, 0.035, 0.048, 0.052, and 0.070 in the same temperature range of the ultrasonic investigation. The measurements were performed using a supermonochromator with a resolution of 700 MHz. In comparison with a Fabry-Pérot interferometer, this apparatus allows a very good reaction of unwanted stray-light contributions, free spectral range superposition, and a high luminosity. The exciting light source was an Ar^+ laser 5145 Å. The scattering measurements were made at a scattering angle $\theta=90°$ with a $\Delta\theta=\pm1°$. The speed of sound was determined from the peak position of the Brillouin doublet and its accuracy is estimated to 1%; the hypersonic damping was evaluated from the full width at half maximum (uncertainty ≈10%).

III. RESULTS

In the water-rich region of concentration BE aqueous solutions exhibit a closed loop of solubility [9]. A recent and accurate determination of the low-temperature portion of the phase diagram [12] enables us to locate the lower critical solution temperature at $T_c=49.2$ °C and $X_c=0.052$ (see Fig. 8).

The concentration and temperature dependence of the ultrasonic (5 MHz) and hypersonic sound velocities at 0, 25, and 45 °C are shown in Figs. 1 and 2. The first plot shows that, as usual in aqueous solutions of short-chain monohydric alcohols [14], the ultrasonic velocity exhibits sharp peak values (c^*) which tend to disappear at high temperatures. However, unlike the other solutions, in BE mixtures the corresponding compositions X_c^* shift toward lower values as T increases. The hypersonic (hs) velocities (c_{hs}) also show peak values (c_{hs}^*) whose compositions ($X_{c,hs}^*$) increase as T decreases. Furthermore,

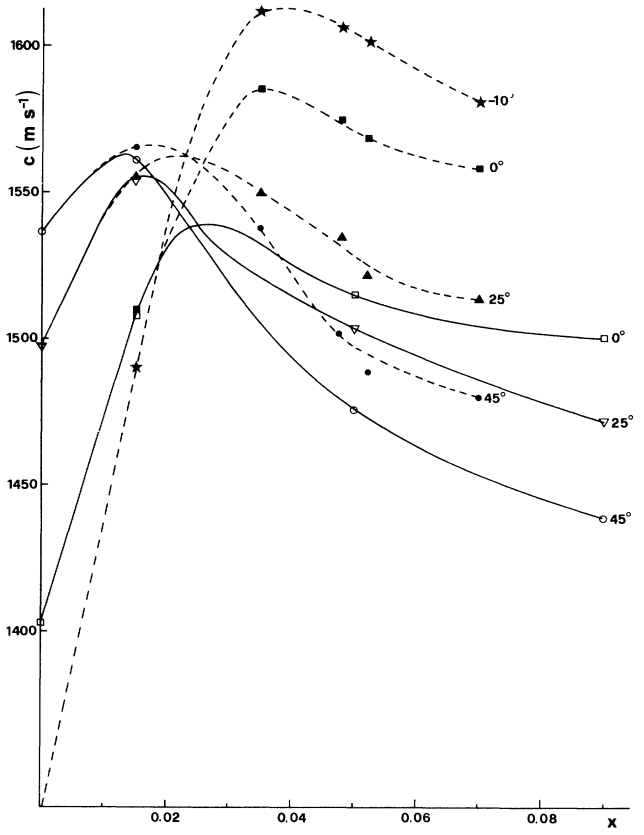

FIG. 1. Ultrasonic (5 MHz, open symbols) and hypersonic (~5.8 GHz, solid symbols) velocity as a function of concentration X (BE mole fraction) for some temperatures. Continuous and dashed lines connecting ultrasonic and hypersonic data, respectively, are drawn for visual purposes.

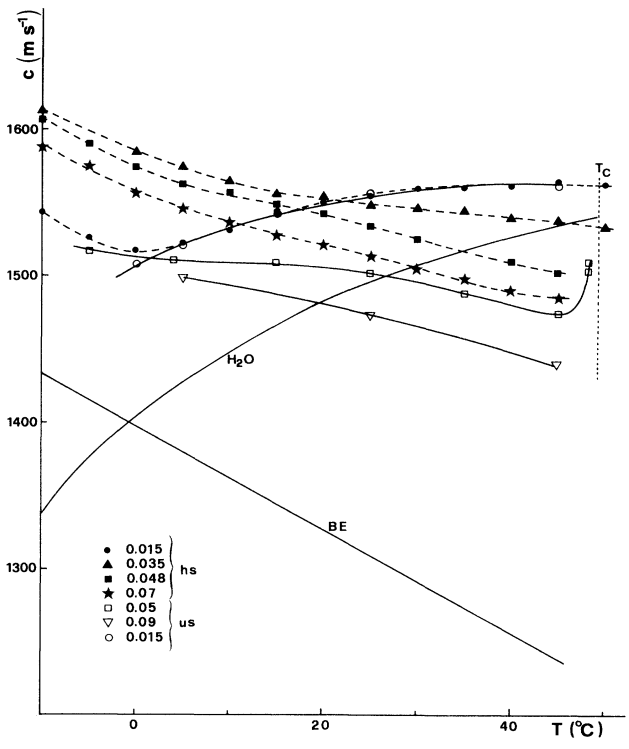

FIG. 2. Ultrasonic (5 MHz, open symbols) and hypersonic (~5.8 MHz, solid symbols) velocity as a function of temperature for some concentrations. Continuous and dashed lines connecting ultrasonic and hypersonic data, respectively, are drawn for visual purposes.

$X^*_{c,\mathrm{hs}} > X^*_c$ and c^*_{hs} display no regular behavior with T. As shown in Fig. 3, these findings are related to the different sound velocity dispersions at various temperatures and concentrations. It is worth noting that for all the temperatures investigated and within the experimental accuracy, the sound velocity dispersion is negligible in the low composition range up to $\sim X^*_c$ [15]. Above this range the velocity dispersion becomes very large and increases as T decreases.

Figures 4–6 show the dependence of the ultrasonic (5 MHz) and hypersonic ($\sim$5.84 GHz) attenuation as a function of X, T, and $\log_{10} f$. From these figures we can note the following characteristic trends.

(a) The attenuation isotherms exhibit peak values $(\alpha/f^2)^*$, which increase noticeably (10^2–10^3 times larger than in pure components) as temperature decreases (see Fig. 4). This behavior is similar to that observed in solutions with monohydric alcohols [16,17] and nonionic C_nE_m surfactants [18]. The increase of the attenuation toward the peak values is very sharp. After an initial region where α/f^2 is weakly dependent on X, it suddenly increases in a narrow concentration range around X^*_c.

(b) The composition (X^*_α) corresponding to the α/f^2 peaks is higher than X^*_c.

(c) The hypersonic attenuation is much lower than the ultrasonic one, thus indicating the occurrence of large relaxational effects. These effects are much larger at the higher concentrations.

(d) At $X=0.015$ the temperature dependence of the ultrasonic attenuation (Fig. 5) is reversed with respect to other concentrations, thus indicating different physical conditions.

(e) At $X=0.05$ (very close to the critical concentration $X_c=0.052$) and for $T\to T_c$, α/f^2 displays a rather smooth increase (see Fig. 5 and Ref. [9]), while the sound velocity exhibits abnormal changes (see Fig. 2 and Ref. [7]). These findings contrast with the behavior usually found in normal binary critical mixtures.

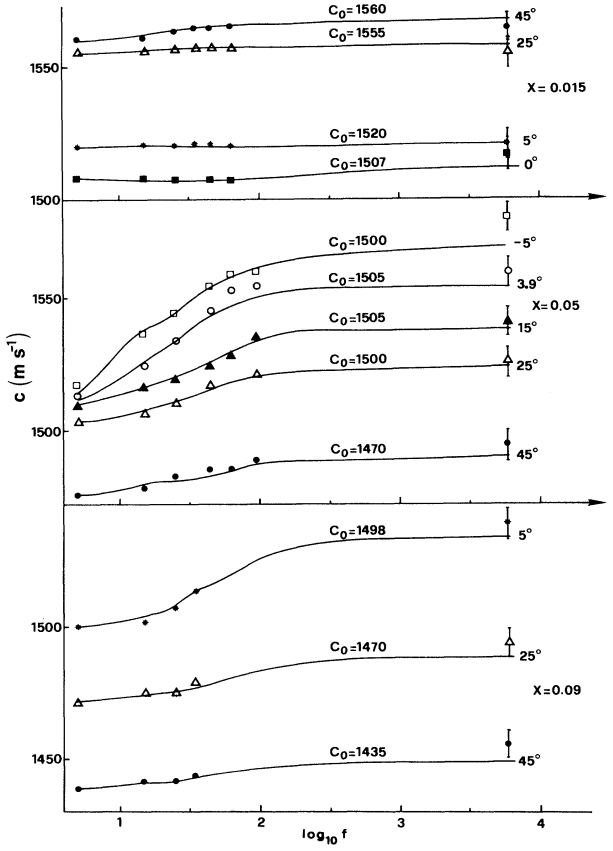

FIG. 3. Sound velocity dispersion for some concentrations and temperatures. Hypersonic values at $X=0.05$ are interpolations between $X=0.048$ and 0.052. Continuous lines are calculated from Eq. (7) in the text by using the parameters obtained in the best fitting of attenuation data to Eq. (2). The reported c_0 (zero-frequency velocity) is the best-fitting free parameter in Eq. (7).

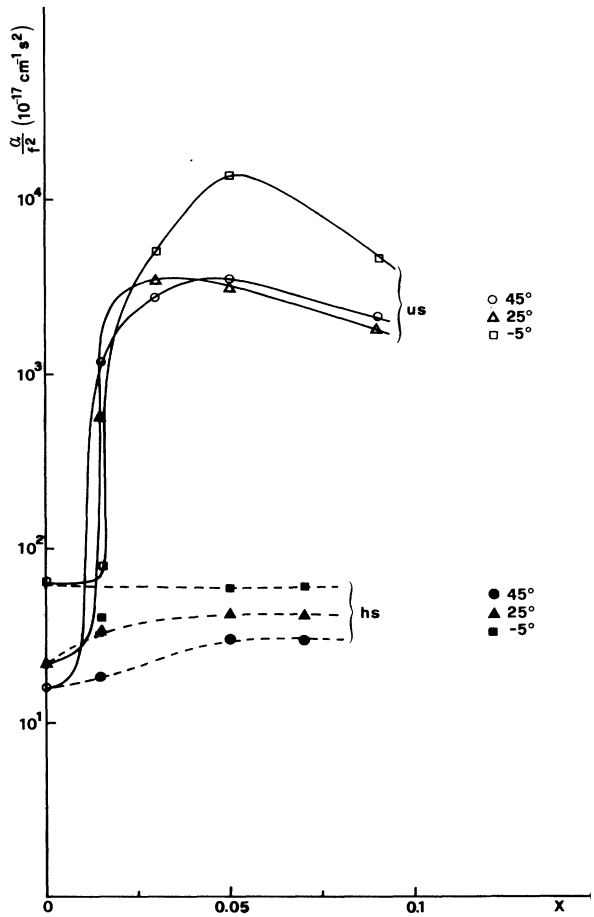

FIG. 4. α/f^2 (in $\log_{10}$ scale) as a function of concentration for some temperatures at 5 MHz (ultrasonic) and $\sim$5.8 GHz (hypersonic). Lines are drawn for visual purposes.

IV. ANALYSIS OF DATA

In order to elucidate the dynamical properties of a system by ultrasonic methods, it is important to obtain accurate relaxation spectra in a wide frequency range. Our ultrasonic absorption measurements were performed at several (9–13) frequencies in the range 5–250 MHz. By considering the hs data at ~5.84 GHz, we cover about three decades of frequency so that the set of experimental points is satisfactory for probing different relaxation equations.

In view of the possible mechanisms responsible for ultrasonic losses in BE aqueous solutions (see Sec. V), we checked our absorption data against the following relaxational behaviors.

(a) Single-relaxation-time equation: In this case the ultrasonic attenuation assumes the form

$$\frac{\alpha}{f^2}=\frac{A}{1+\omega^2\tau^2}+B \ , \tag{1}$$

where $\omega=2\pi f$, $\tau=(2\pi f_R)^{-1}$ is the relaxation time and f_R the corresponding frequency, A is the amplitude, and B is a contribution at frequencies well above the investigated range. The corresponding excess sound absorption per wavelength is

$$(\alpha\lambda)_{\rm exc}=\left[\frac{\alpha}{f^2}-B\right]f_R c=\frac{A}{1+\omega^2\tau^2}f_R c \tag{1'}$$

with a maximum value (strength) given by

$$\mu=(\alpha\lambda)^*_{\rm exc}=Af_R c/2 \ . \tag{1''}$$

(b) Two-relaxation-time equation:

$$\frac{\alpha}{f^2}=\frac{A_1}{1+\omega^2\tau_1^2}+\frac{A_2}{1+\omega^2\tau_2^2}+B \ . \tag{2}$$

The strengths corresponding to the two processes are given by

$$\mu_1=A_1 f_{R1}c/2, \quad \mu_2=A_2 f_{R2}c/2 \ . \tag{2''}$$

Equations (1) and (2), or, in general, discrete distributions of relaxation times, are predicted by the so-called quasichemical models where sound attenuation is related to association reactions (see Sec. V).

(c) Romanov-Solovyev (RS) equation (Ref. [19]) (concentration-fluctuation model):

$$\frac{\alpha}{f^2}=A_{\rm RS}(X,T)F_{\rm RS}(\omega^*)+B \ . \tag{3}$$

In this equation the ultrasonic attenuation is related to the perturbation of concentration fluctuations produced by the passage of sound waves. $A_{\rm RS}(X,T)$ is an amplitude and $F_{\rm RS}(\omega^*)$ is a known [17] scaling function coming from the assumption of a continuum (Debye) distribution of diffusive relaxation times $\tau_q=(2Dq^2)^{-1}$ associated with the decay of each q component of the spatial fluctuations spectrum. In these relations D is the diffusion coefficient and $\omega^*=\omega/\omega_M$, where $\omega_M=2Dq^2_{\rm max}$ is a characteristic maximum frequency of fluctuations (see Sec. V).

(d) Ferrell-Bhattacharjee (FB) equation (Refs. [20,9]) (critical attenuation):

$$\frac{\alpha}{f^2}=A_{\rm FB}(X,T)F_{\rm FB}(\omega^*)+B \ . \tag{4}$$

This equation properly describes the ultrasonic attenuation in binary critical mixtures as due to the coupling of sound waves to critical concentration fluctuations. $A_{\rm FB}(X,T)$ is an amplitude, $F_{\rm FB}(\omega^*)=\omega^*/(1+\omega^{*0.5})^2$ is a scaling function, and $\omega^*=\omega/\omega_D$, where $\omega_D=2D\xi^{-2}$ is a characteristic relaxation rate associated with energy fluctuations and ξ the correlation length of the system. We check Eq. (4), which is valid for critical mixtures, since the low-T ultrasonic behavior in alcohol solutions resembles that observed near a demixing point of a binary critical mixture and, in addition, our high-T absorption measurements extend to about 4 °C from T_c.

(e) Cole-Davidson (CD) distribution (Ref. [21]):

$$\frac{\alpha}{f^2}=A_{\rm CD}\frac{\cos^\beta\theta\sin(\beta\theta)}{\omega}+B \ , \tag{5}$$

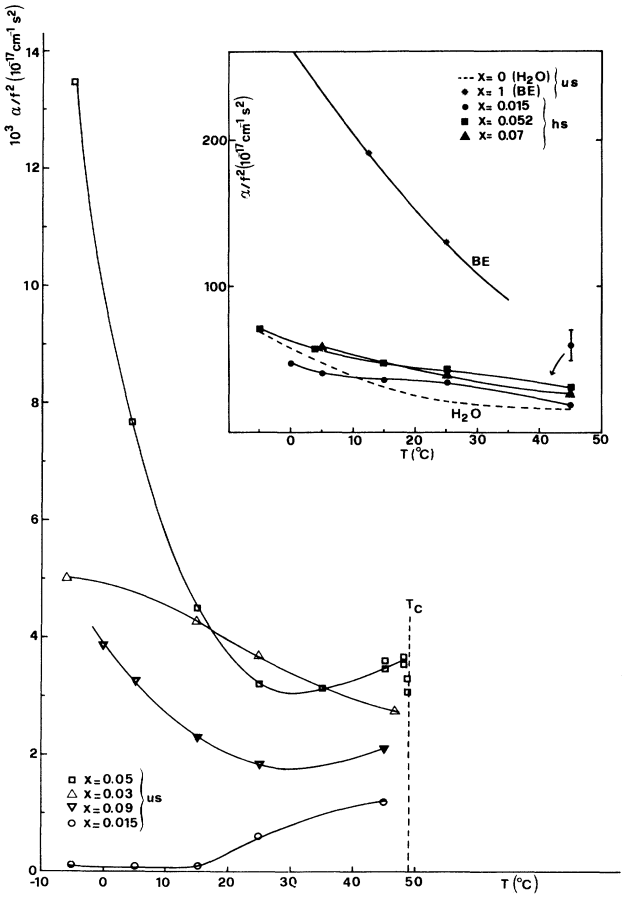

FIG. 5. Ultrasonic attenuation (α/f^2) at 5 MHz as a function of temperature for some concentrations. Inset: the same plot (different scale) in pure components and for hypersonic data as in the investigated solutions.

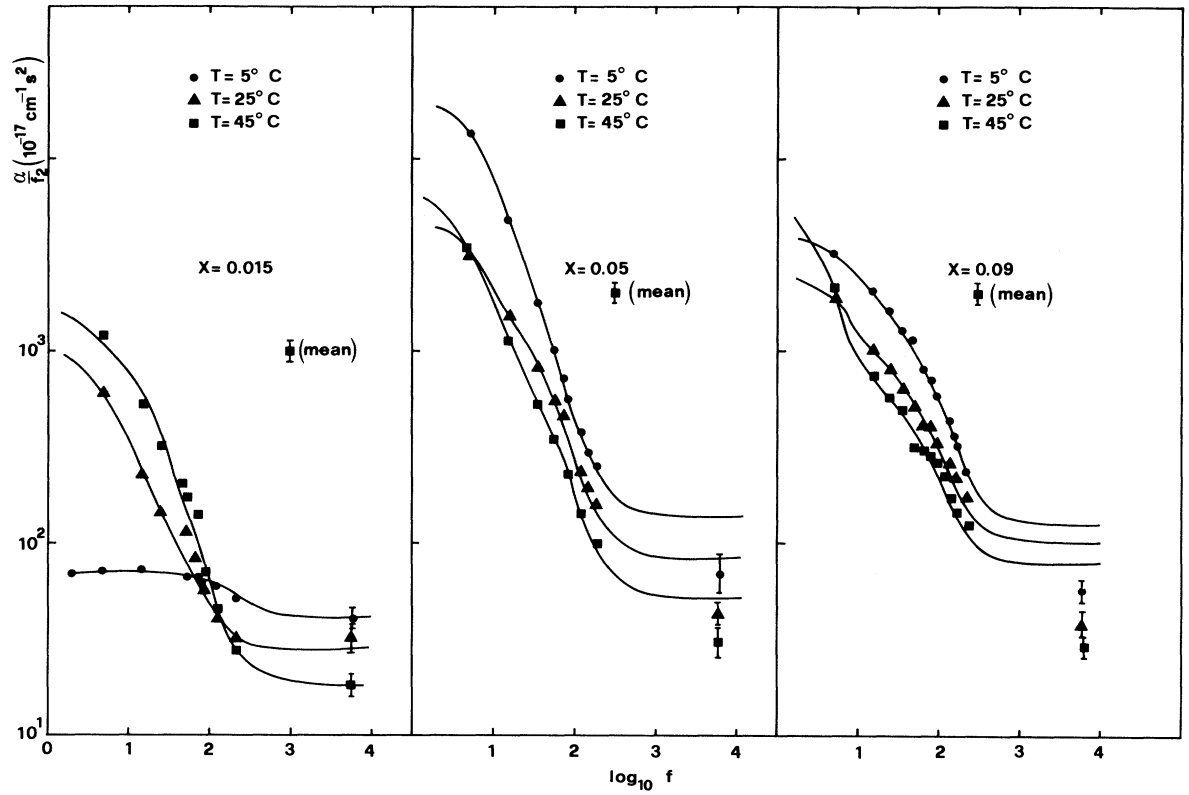

FIG. 6. Log-log plot of the sound attenuation (α/f^2) as a function of frequency for some concentrations and temperatures. Lines are best-fitting curves to the two-relaxation times Eq. (2) with parameters reported in Table I.

where $\theta=\arctan\omega\tau$, and β and τ are parameters characterizing the width and the maximum relaxation time in the asymmetrical Cole-Davidson distribution. The use of Eq. (5) is suggested from the possibility that a structural relaxation (i.e., frequency-dependent compressional and shear elastic moduli) takes place in our system as a consequence of aggregation phenomena. Similar effects have been found, for example, in micelle-forming binary systems [22]. For $\beta=1$ Eq. (5) reduces to Eq. (1).

(f) Approximate Cole-Cole distribution (stretched form) (Ref. [22]):

$$\frac{\alpha}{f^2}=\frac{A}{1+(\omega\tau)^{2(1-\alpha)}}+B\ . \tag{6}$$

Arguments similar to those in item (e) suggest the use of this equation. For $\alpha=0$, Eq. (6) reduces to Eq. (1).

We first fitted our ultrasonic and hypersonic absorption data to Eqs. (1)–(6). For this purpose we used a computer least-squares procedure which gives for each spectrum the set of parameters ($A_i,\tau_i,B,...$) of each equation, which minimizes the root-mean-square (rms) deviation. The reliability of each equation to fit a spectrum was established by comparing the corresponding rms minima and taking into account the number of free parameters in each equation. By using this criterion we found that all the attenuation spectra are, in general, better accounted for by discrete relaxation equations [Eq. (1) or (2)] rather than by the continuous ones [Eqs. (3)–(6)]. For the sake of comparison and in view of the discussion in Sec. V, we show in Table I the fitting parameters and the rms minima corresponding to Eq. (2) and to the RS equation (3). Some fittings of the experimental points to Eq. (2) are shown in Fig. 6. In particular, the results from the fitting can be summarized as follows.

(i) $X=0.015$: At high temperatures ($T\geq 25\,^{\circ}C$) these samples display a two-relaxation-time behavior (fast and slow processes), but for $T<25\,^{\circ}C$ the attenuation data can be described either by a single (fast) process, Eq. (1), or by the RS equation (3).

(ii) $X\geq 0.03$: The ultrasonic spectra in these samples over the whole temperature range conform to Eq. (2). [Note: For $X>0.03$ the hypersonic data lie systematically down the fitting curves (see Fig. 6). This finding indicates the presence of additional relaxation processes above $\sim$300 MHz. However, the strengths of such processes are so small (take into account the logarithmic scale in Fig. 6) that we can neglect them for further discussions.] Even if for some temperature it happens that the quality of the fit (rms minimum) to one of the remaining equations [(1), (3)–(6)] is comparable to that of Eq. (2), this finding looks casual and not systematic, as Eq. (2) does. Table 1 of Ref. [9] shows that the ultrasonic spectra in samples $X=0.03$ and 0.09 exhibit a best fitting to Eq. (2) and sometimes to Eqs. (3) and (4). However, these

TABLE I. Best-fitting parameters to the single and double relaxation equation (2) and to the RS equation (3). [f (MHz); A,B (10^{-17} cm^{-1} s^2).]

T (°C)	f_l	f_h	f_M	A_l	A_h	A_{RS}	B Eq. (2)	B Eq. (3)	rms Eq. (2)	rms Eq. (3)
					$x=0.015$					
45	8	41	24	1314	253	2309	18	30	4.5	17.3
25.2	6	50	17	833	91	1335	28	38	2.5	11.5
15.1		52	112		45	73	36	35	2.1	1.8
5		216	658		27	38	41	40	2.9	2.3
0.15		370	2205		33	40	45	44	4	3.5
					$x=0.03$					
50.3	16	73	46	1335	290	2372	36	66	16.7	20.3
47	7	54	22	3240	574	5344	33	121	13.5	77
25	9	49	28	3716	837	6601	41	102	10.4	59.1
					$x=0.05$					
45.2	5	50	14	5758	558	8860	52	139	10.2	77.1
35.1	4	48	17	5869	829	6946	64	208	7.7	106
25	6	45	29	3492	1072	5429	84	174	29.5	97.6
14.9	5	42	27	5693	1589	7929	87	210	20.6	132.8
3.9	8	38	26	7732	2053	14 106	108	220	25.6	128.9
−5	7	39	16	17 607	1735	32 115	139	301	40.2	142.7
					$x=0.09$					
45	3	63	19	5784	474	4188	78	154	25	76.2
25	6	65	50	1753	685	2401	102	160	21.6	67.3
5	9	61	63	2308	1388	4295	126	183	30.5	76.2

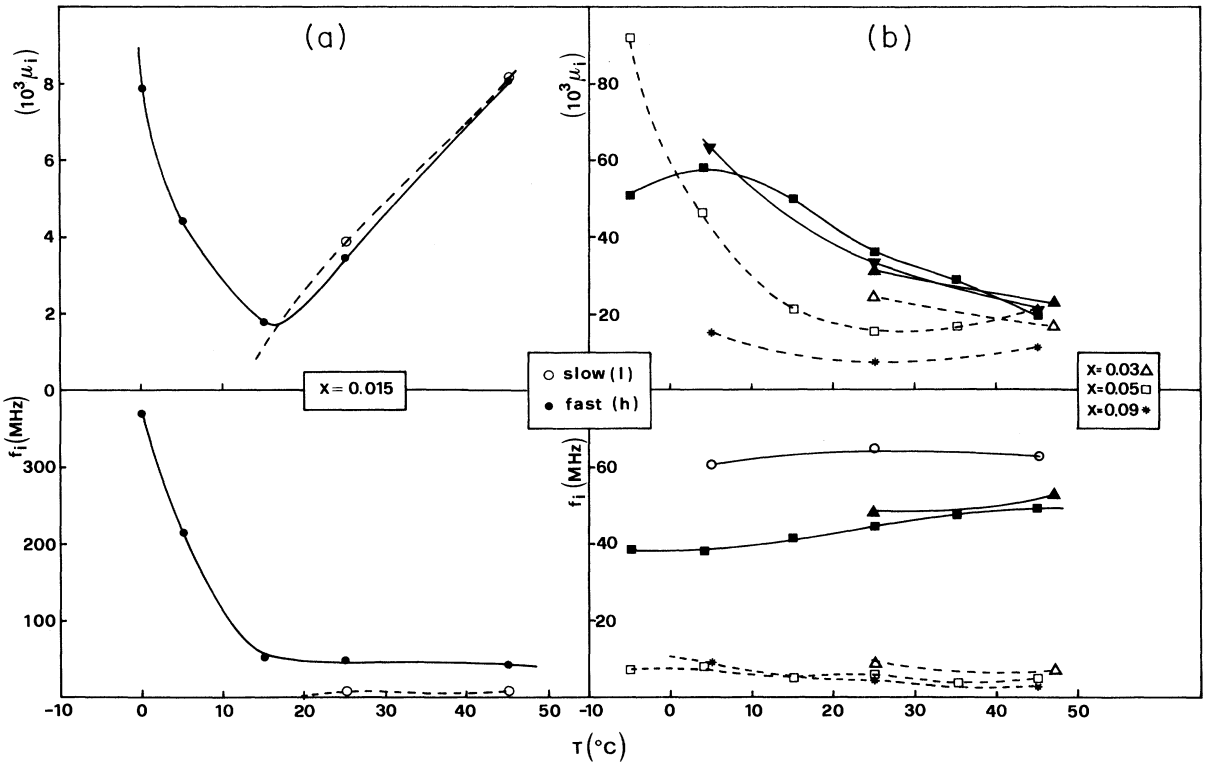

FIG. 7. Temperature dependence of the strengths (μ) and relaxation frequencies (f) at (a) $X=0.015$ and (b) $X \geq 0.03$. Continuous lines connecting solid symbols refer to the fast (h) process, dashed lines and open figures to the slow (l) one. Lines are drawn for visual purposes. Note the different scale in the two figures.

data, when reanalyzed taking into account the additional hypersonic data, show undoubtable best agreement to Eq. (2). Strengths and relaxation frequencies of the fast and slow processes as a function of T are shown in Figs. 7(a) ($X=0.015$) and 7(b) ($X \geq 0.03$).

In order to have a further check on the assignment of our relaxation spectra to a single- or double-time equation and on the related parameters μ_i and f_i, we performed a self-consistency test by using the sound velocity data as a function of frequency. The sound velocity dispersion corresponding to Eq. (2) is given by

$$c^2(\omega) \cong c_0^2 \left[1 + \frac{2}{\pi} \left[\mu_1 \frac{\omega^2 \tau_1^2}{1+\omega^2 \tau_1^2} + \mu_h \frac{\omega^2 \tau_h^2}{1+\omega^2 \tau_h^2} \right] \right], \quad (7)$$

where c_0 is the sound velocity in the limit $\omega \rightarrow 0$ and it is assumed that $[c^2(\infty)-c_0^2]/c_0^2 \ll 1$. A similar equation holds for single relaxation. By using the parameters μ_i and $\tau_i=(2\pi f_i)^{-1}$, previously obtained in the absorption fits, and taking c_0 as a free parameter, we calculated the sound velocity curves Eq. (7). The good agreement with experimental points is shown in Fig. 3.

V. DISCUSSION

There is little doubt that the peculiar concentration and temperature behavior of ultrasonic propagation in aqueous solutions with alcohols is attributable to relaxation processes connected with molecular associations [16]. There are at present two kinds of models describing the ultrasonic relaxation due to the nonrandom distribution of concentration in binary mixtures. In the so-called quasichemical models [23,24], the formation of stable intermolecular groups (complexes), whose equilibria are perturbed by sound waves, is assumed. Strength and relaxation frequency corresponding to this mechanism are related to a relaxational compressibility [which depends on the volume (ΔV) and enthalpy (ΔH) changes of the reaction] and to the reaction rates, respectively.

The quasichemical approaches have been severely criticized [25,26,16] on the grounds of physical reasons since they assume the existence of stable complexes of definite size rather than a more realistic distribution of sizes or multistep reactions. In addition, even if the thermodynamic and kinetics parameters involved in the reactions can be determined from the experimental ultrasonic data, it is not clear whether they have a real physical meaning since they cannot be evaluated independently.

The concentration fluctuation approach [19] to sound propagation in nonuniform binary mixtures eliminates some of the previous problems. The shift of the equilibrium of concentration fluctuations due to the temperature and pressure changes associated to sound waves leads to relaxational volume (ΔV) and enthalpy (ΔH) contributions. Since each q component of the Fourier expansion of concentration fluctuations decays with a relaxation time $\tau_q=(2Dq^2)^{-1}$, one obtains a distribution of relaxation times extending from infinity to a minimum $\tau_{\min}=(2Dq_{\max}^2)^{-1}=(l_{\min}^2/2D)$, where $q_{\max}$ is a q cutoff associated with a minimal fluctuation size $l_{\min}$ (Debye cutoff). The analytical form of the sound attenuation from this approach is given by the Romanov-Solovyev equation (3), where the amplitude $A_{RS}(X,T)$ is related to D, $l_{\min}$, and to a complex thermodynamic parameter which depends on the second derivative of V, H, and free-energy G of the mixture. Although the amplitude can in principle be evaluated independently, the lack and/or the accuracy of thermodynamic data make the comparison with the experimentally obtained $A_{RS}(X,T)$ very difficult. For this reason, the comparison of the experimental data to the fluctuation model is usually restricted to the analysis of the frequency dependence.

As shown in Sec. IV, our ultrasonic spectra in more concentrated solutions ($X \geq 0.03$) are well accounted for by a two-relaxation-time equation. Such a result allows us to exclude the possibility that concentration fluctuation models can explain the ultrasonic spectra in such systems, because they predict a continuum distribution of relaxation times. Furthermore, we can give an additional argument against the RS model. As previously discussed, this model predicts a maximum relaxation frequency $f_M=D/\pi l_{\min}^2$, where $l_{\min}$ is an unknown parameter which would be of the order of intermolecular spacings [19] (2–5 Å). We compared the parameter f_M obtained by the best fitting to Eq. (3) at $X=0.05$ and different temperatures (see Table I) with independent evaluations of D and $l_{\min}$. For this purpose we used the experimental D recently obtained by quasielastic light-scattering (QELS) experiments [12] ($D=3.5\times10^{-7}$, 6.4×10^{-7}, 4.8×10^{-9}, and 1.5×10^{-9} cm^2 s^{-1} at $T=45$, 25, 15, and 5 °C, respectively) and taken to be $l_{\min}=\xi$, where ξ is the correlation length ($\xi=60$, 15, 12, and 8 Å) of the centers of scattering in SANS experiments [13]. With these values we get $D/\pi l_{\min}^2=0.32$, 9, 0.09, and 0.08 MHz. By comparing these values with the fitted f_M in Table I, we can see that, apart from the value at 25 °C, the order of magnitude of $D/\pi l_{\min}^2$ is much lower than f_M. Even taking for $l_{\min}$ a reasonable value of 5 Å, we find again $D/\pi l_{\min}^2 \ll f_M$. Thus we can conclude that the relaxation frequencies observed in our samples in the investigated frequency range ($f \geq 5$ MHz) are not related to concentration fluctuations whose contribution, if any, lies below the experimental frequency range. An opposite conclusion was found in solutions with short-chain alcohols such as ethanol [17] and 1-propanol [27].

As previously noticed, the interpretation of the ultrasonic spectra on the grounds of chemical association reactions poses some physical problems. However, the nonequivocal discrete distribution behavior indicates that specific relaxation processes are responsible for the observed ultrasonic dynamics. We will show in the following that the concentration and temperature dependence of the ultrasonic behavior, as well as the indications from other sources, allow us to assign the underlying relaxational processes to peculiar association reactions.

An inspection of the concentration dependence of the sound velocity and absorption (Figs. 1 and 4) shows that our system is characterized by three concentration ranges. The first, which extends from $X=0$ to about $X=X_c^*$, is characterized by the sudden increase of the sound velocity in contrast with the almost insensitivity of

the sound attenuation and absence of significant dispersion effects. Then, in a narrow concentration range around X_c^*, the ultrasonic velocity inverts its increasing trend, while the ultrasonic absorption exhibits an abrupt increase accompanied by noticeable relaxation effects up to X_α^*. The range $X_c^* \leq X \leq X_\alpha^*$ then corresponds to a second characteristic concentration region, while for $X > X_\alpha^*$ (the third region) the anomalous ultrasonic behavior starts to disappear.

The abrupt changes around X_c^* clearly reflect some structural modification in the system. This finding is confirmed by the behavior of several other properties which have been reviewed by Kilpatrick *et al.* [28]. According to these authors, many experiments in BE plus water solutions indicate that there exists a narrow concentration range ($0.016 \leq X \leq 0.021$ at 25 °C) beyond which BE molecules self-aggregate, giving rise to "microphases" of micellelike BE-rich and water-rich domains. A similar conclusion was reached by Ito *et al.* [10,11] by interpreting Rayleigh scattering spectra and by Kato [29] by evaluating the Kirkwood-Buff parameters of the mixtures. More direct evidence for BE aggregations is given by recent SANS [13] and light-scattering experiments [12]. According to the above indications, we consider the narrow concentration range around X_c^* as reminiscent of the critical micelle concentration (CMC) of a binary surfactant system. By plotting the temperature dependence of X_c^* from Fig. 1, we obtained the CMC-like curve of BE aqueous solutions shown in Fig. 8.

The existence of a CMC-like curve implies that in solutions where $X < X_{\mathrm{CMC}}$ the alcohol molecules are not aggregated but monomolecularly dispersed in the water while for $X > X_{\mathrm{CMC}}$ (where X_{CMC} represents the value of the critical micelle concentration), alcohol aggregates are formed. With reference to Fig. 8, we can see that our samples of $X=0.015$ at $T < 25$ °C are located below the CMC-like curve, while the remaining solutions are always above this curve. As shown in Sec. IV these two groups of solutions are characterized by different behaviors. In fact, the ultrasonic spectra in the first group are accounted either by a single time Eq. (1) or by the RS equation (3), while a double (fast and slow processes) relaxation is observed in the second one. However, the values of the relaxation frequencies from Eq. (1) in the first group of solutions (see Table I) suggest a physical continuity with the fast process found in the remaining samples so that we will associate the spectra at $X=0.015$ and $T < 25$ °C to a single (fast) relaxation. This assumption, even if unnecessary, allows us to rationalize the overall experimental ultrasonic behavior by assigning the fast-relaxation process to equilibria of type

$$A + W_m \rightleftharpoons AW_m \rightleftharpoons (AW_m)_n \tag{8}$$

and the slow one to the alcohol self-association reaction

$$rA \rightleftharpoons A_r \ , \tag{9}$$

where W and A are water and alcohol monomers, respectively, and W_m, A_r, AW_m, and $(AW_m)_n$ molecular complexes. Similar assignments have been made in previous ultrasonic studies in water solutions with alcohols of large hydrophobic groups (1-propanol [30], *t*-butanol [24,31], 2-*n*-butoxyethanol [6,8], 2-iso-butoxyethanol [32]). However, these studies were limited to $T=25$ °C and do not allow for testing the role of temperature on the alcohol aggregation phenomena.

The absence of aggregates for $X < X_{\mathrm{CMC}}$ does not mean that single alcohol molecules do not affect the structural properties of water. On the contrary, as shown by the sudden increase of the sound velocity as well as by the behavior of other physical properties [33], BE molecules modify the tethraedrical network of water. Such modifications are usually explained on the grounds of structural models [14]. The most frequently used model is the clathrate-hydrate model where each alcohol molecule is supposed enclathrated in a water cage. At higher concentrations, where the amount of water is insufficient to accommodate all the alcohol molecules in a single water cage, two or more alcohol molecules can enter a merged clathrate. According to Tamura, Maekawa, and Yasunaga [24], and depending on the concentration, we then associate the fast-relaxation process to association reactions of type Eq. (8) where (AW_m) and $(AW_m)_n$ are clathrate hydrates and merged clathrates, respectively.

Let us consider the temperature dependence of the strengths (μ_i) and relaxation frequencies (f_i) of the two processes at $X=0.015$ [see Fig. 7 (a)]. These parameters display a different behavior below and above 25 °C. For $T < 25$ °C the slow process is absent and the frequency f_h of the fast one takes very high values at low T. By contrast, for $T \geq 25$ °C both f_l and f_h take approximately the values found in more concentrated solutions [Fig. 7(b)].

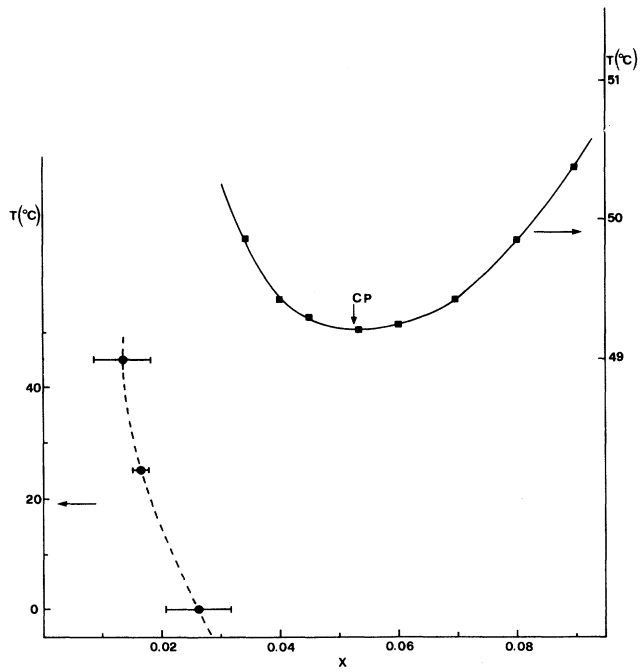

FIG. 8. Coexistence curve (low-T portion) of BE-water solutions and the related CMC-like curve (dashed line) as obtained from the ultrasonic velocity maxima in Fig. 1.

According to our assignments, these findings indicate that, for $T<25\,^{\circ}C$, the alcohol aggregation is negligible, whereas for $T\geq 25\,^{\circ}C$ it gives a (small) contribution to the sound absorption. Since, in first approximation, the relaxation frequencies involved in chemical equilibria depend on the concentration of the species, whereas the corresponding strengths depend on the volume change (approximately the size of the aggregates), we can understand the large increase of f_h at low T as due to the increased concentration of clathrate structures when the alcohol molecules are not aggregated. By contrast, the concentration of clathrates decreases at high T where alcohol aggregation takes place.

In the more concentrated solutions ($X\geq 0.3$) both processes are present and their characteristic frequencies ($f_l\approx 6-9$ MHz, $f_h\approx 40-60$ MHz) slightly depend on X and T being of the same order of magnitude as those at $X=0.015$ and high T [see Fig. 7(b)]. These findings again support the coexistence of alcohol and clathrate aggregates. However, the strengths of both processes are much higher than at $X=0.015$. According to our interpretation it means that the aggregates are much larger taking a maximum value at $X=0.05$.

The low-T behavior of two processes in the samples $X\geq 0.03$ deserves some discussion. Comparing Fig. 4 and Fig. 7(b) we can see that the noticeable increase of the attenuation peak at $X_\alpha^*\approx 0.05$ as T decreases is related to the large increase of both μ_l and μ_h. We must observe, however, that the presence of peak values in the plot α/f^2 vs X and their anomalous increase at low temperatures is not peculiar to solutions with associating alcohols (such as 1-propanol. t-butanol, and butoxyethanols). As known, these characteristic features are also observed in solutions with short monohydric alcohols [9,17] or alcohols containing small hydrophobic groups (e.g., 2-propanol [34], allyl-alcohol [31], 2-propoxyethanol [35]) where ultrasonic spectra exhibit a single-relaxation behavior or conform to concentration fluctuation models. On the other hand, SANS studies [13] in these systems confirm the absence of alcohol aggregates, so that their ultrasonic peak values must be related to the fast process. From Fig. 7(b) we can see that μ_l and μ_h are of the same order of magnitude and both noticeably increase as T decreases. This observation can explain why the α/f^2 peak values in solutions with nonassociating alcohols take values lower than those in the associating ones (see Fig. 6 in Ref. [9]).

According to our picture, the very large increase of μ_h and μ_l in low-T solutions should be associated to the growth of large clathrate (or merged clathrates) structures and alcohol aggregates, respectively. Apparently this conclusion disagrees with SANS experiments [13], which show the presence of large BE aggregates whose size monotonically decreases as T decreases. However, recent QELS experiments [12] show noticeable increases of both scattered intensity and mean hydrodynamic radii (up to ~ 2000 Å) for $0.03\leq X<0.07$ as the temperature decreases below $\sim 25\,^{\circ}C$. This apparent contradiction with SANS results was ascribed to the different scale lengths probed by neutron- and light-scattering experiments and interpreted as due to an interaction process among micellelike alcohol aggregates that gives rise to the formation of large clusters of correlated micelles. The presence of these structures can explain the large increase of the low-frequency ultrasonic strength μ_l at low T. The microscopic picture of BE solutions at low T emerging from the above analysis is then that of systems containing large water-rich and alcohol-rich domains as if it were a microscopic unmixing. Similar conclusions have been found previously by means of different experiments in BE [11,29] and t-butano [36] solutions.

One last point deserves discussion. Since BE can be considered as a short homolog (C_nE_1) of larger nonionic surfactants C_nE_m, we can compare the ultrasonic behavior in our system with that in C_nE_m micellar aqueous solutions. Borthakur and Zana [18], by investigating solutions with C_6E_3, C_6E_5, and C_8E_6, found a behavior quite similar to that in our BE solutions. In particular, they observed the characteristic α/f^2 vs X peaks (which increase as temperature decreases) as well as a slow- (2–6 MHz) and a fast-relaxation processes. They ascribed the two processes to a surfactant exchange reaction in the micelles [as in Eq. (9)] and to an equilibrium between "surfactant bond" water molecules and free-water molecules, respectively. This analogy supports that alcohol aggregates in BE solutions are micellelike, as suggested in Refs. [1,28,12].

The similarity of the ultrasonic propagation in nonionic surfactants and in BE solutions becomes very striking as the critical behavior is concerned. In contrast to the molecular binary critical mixtures, in both systems the critical divergence of the ultrasonic attenuation as a function of temperature looks, in fact, very smooth near the critical point (see Fig. 5 and Ref. 18]) and the sound velocity display in our system an abrupt increase (see Fig. 2). These findings call for further detailed experiments near the critical point, but they seem to be related to the micellization processes occurring in these systems. We have shown previously that the presence of large-scale aggregates limits the characteristic frequency of concentration fluctuations ($f_M=D/\pi\xi^2$) to values below the frequency range of ultrasonic experiments, so that in this range one mainly detects the slow and fast processes associated to clathrates and alcohol aggregates. The persistence of such aggregates up to the critical temperature, can maintain low f_M even in the proximity of the critical point. Under these conditions, the smooth increase of α/f^2 for $T\rightarrow T_c$, shown in Fig. 5, can be due to a contribution from the high-frequency tail of the critical concentration fluctuations.

VI. CONCLUSION

To explain the concentration, temperature, and frequency behavior of the ultrasonic velocity and absorption measured in concentrated BE aqueous solutions we assumed the coexistence of water-rich (clathrate hydrates) and alcohol-rich (micellelike) domains. This assumption is supported by the concentration dependence of the ultrasonic properties, by the unequivocal double-relaxational behavior of the spectra, and by several re-

sults from other experiments. An independent quantitative analysis of the characteristic frequencies of concentration fluctuations shows that contributions to sound absorption from this mechanism lie in a frequency range below the one investigated.

From our assumptions and from the overall temperature and concentration behavior of the sound propagation, we found that at low temperatures the size of the clathrate structures grows, while the small micellelike alcohol aggregates are likely to interact together giving rise to very large clusters of correlated particles. The apparent lack of critical divergence of the sound absorption at high temperatures near the critical point is explained as due to large noninteracting micellelike aggregates which limit the characteristic frequency of concentration fluctuations to values below the frequency range of ultrasonic experiments.

ACKNOWLEDGMENTS

We thank Dr. J. Teixeira of CEN Saclay (France) for useful discussions concerning SANS data. The financial support to three of the authors (G.D., F.M., and A.P.) comes from Gruppo Nazionale di Struttura della Materia and Centro Interuniversitario Struttura della Materia del Ministero della Pubblica Istruzione.

[1] G. Roux, G. Perron, and J. E. Desnoyers, J. Phys. Chem. **82**, 966 (1978).
[2] G. Roux, G. Perron, and J. E. Desnoyers, J. Solution Chem. **7**, 639 (1978).
[3] S. Harada, T. Nakajima, T. Komatsu, and T. Nakagawa, J. Solution Chem. **7**, 463 (1978).
[4] C. J. Burton, J. Acoust. Soc. Am. **20**, 186 (1948).
[5] J. Lara and J. Desnoyers, J. Solution Chem. **10**, 465 (1981).
[6] S. Nishikawa, M. Tanaka, and M. Mashima, J. Phys. Chem. **85**, 686 (1981).
[7] S. Nishikawa and K. Kotegawa, J. Phys. Chem. **89**, 2896 (1985).
[8] S. Kato, D. Jobe, N. P. Rao, C. H. Ho, and R. E. Verral, J. Phys. Chem. **90**, 4167 (1986).
[9] G. D'Arrigo and A. Paparelli, J. Chem. Phys. **91**, 2587 (1989).
[10] N. Ito, K. Saito, T. Kato, and T. Fujiyama, Bull. Chem. Soc. Jpn. **54**, 991 (1981).
[11] N. Ito, T. Fujiama, and Y. Udagawa, Bull. Chem. Soc. Jpn. **56**, 379 (1982).
[12] G. D'Arrigo, F. Mallamace, N. Micali, A. Paparelli, J. Teixeira, and C. Vasi, Prog. Colloid Polym. Sci. **84** (1991); F. Mallamace, N. Micali, C. Vasi, and G. D'Arrigo, Phys. Rev. A **43**, 5710 (1991).
[13] G. D'Arrigo and J. Teixeira, J. Chem. Soc. Faraday Trans. **86**, 1503 (1990).
[14] G. D'Arrigo and A. Paparelli, J. Chem. Phys. **88**, 405 (1988).
[15] In the very low T range at $X=0.015$ a velocity dispersion that increases as T decreases is observed (see Figs. 1 and 3). This behavior is similar to that observed in diluted ethanol solutions [O. Conde, J. Teixeira, and P. Papon, J. Chem. Phys. **76**, 3747 (1982)], and it is likely related to the anomalies of supercooled water.
[16] M. J. Blandamer, in *Water. A Comprehensive Treatise,* edited by F. Franks (Plenum, New York, 1973), Vol. 2, Chap. 3; M. J. Blandamer and D. Waddington, Adv. Molec. Relaxation Processes **2**, 1 (1970).
[17] G. D'Arrigo and A. Paparelli, J. Chem. Phys. **88**, 7687 (1988).
[18] A. Borthakur and R. Zana, J. Chem. Phys. **91**, 5957 (1987).
[19] V. P. Romanov and V. A. Solov'ev, Akust. Zh. **11**, 84 (1965) [Sov. Phys. Acoust. **11**, 68 (1965); **11**, 257 (1965) [**11**, 219 (1965)].
[20] R. A. Ferrell and j. Bhattacharjee, Phys. Rev. B **24**, 4095 (1981); J. Bhattacharjee and R. A. Ferrel, Phys. Rev. A **24**, 1643 (1981).
[21] R. Meister, C. J. Marhoffer, R. Sciamanda, L. Cotter, and T. A. Litovitz, J. Appl. Phys. **31**, 854 (1960).
[22] C. Cametti, P. Codastefano, G. D'Arrigo, P. Tartaglia, J. Rouch, and S. H. Chen, Phys. Rev. A **42**, 3421 (1990).
[23] J. H. Andreae, P. D. Edmonds, and J. F. McKellar, Acustica **15**, 74 (1965).
[24] K. Tamura, M. Maekawa, and T. Yasunaga, J. Phys. Chem. **81**, 2122 (1977).
[25] V. A. Solovyev, C. J. Montrose, M. H. Watkins, and T. A. Litovitz, J. Chem. Phys. **48**, 2155 (1968).
[26] G. Atkinson, S. Rajagopalan, and B. L. Atkinson, J. Phys. Chem. **85**, 733 (1981).
[27] W. M. Madigosky and R. W. Warfield, J. Chem. Phys. **86**, 1491 (1987).
[28] P. K. Kilpatrick, H. T. Davis, L. E. Scriven, and W. G. Miller, J. Colloid Interface Sci. **118**, 270 (1987).
[29] T. Kato, J. Phys. Chem. **88**, 1248 (1984).
[30] S. Nishikawa, M. Mashima, and T. Yasunaga, Bull. Chem. Soc. Jpn. **48**, 661 (1975).
[31] S. Nishikawa, M. Mashima, M. Maekawa, and T. Yasunaga, Bull. Chem. Soc. Jpn. **48**, 2353 (1975).
[32] S. Nishikawa and T. Uchida, J. Solution Chem. **12**, 771 (1983).
[33] F. Franks and J. E. Desnoyers, in *Water Science Review 1,* edited by F. Franks and J. E. Desnoyers (Cambridge University Press, London, 1985), pp. 171–232.
[34] S. Nishikawa, M. Mashima, and T. Yasunaga, Bull. Chem. Soc. Jpn. **49**, 1413 (1976).
[35] S. Nishikawa, Y. Yamashita, and M. Mashima, Bull. Chem. Soc. Jpn. **55**, 1 (1982).
[36] G. W. Euliss and C. M. Sorensen, J. Chem. Phys. **80**, 4767 (1984).